ChemComm

Accepted Manuscript

ROYAL SOCIETY OF CHEMISTRY

rsc.li/chemcomm

ChemComm

View Article Online
DOI: 10.1039/C6CC08808B

COMMUNICATION

A novel aggregation-induced emission enhancement triggered by the assembly of chiral gelator: From non-emissive nanofibers to emissive micro-loops

Received xx xx ,
Accepted xx xx

DOI: 10.1039/x0xx00000x

www.rsc.org/

Wenrui Chen,[‡a] Guangyan Qing [‡a] and Taolei Sun[*ab]

In this study, a novel aggregation-induced emission (AIE) enhancement triggered by the self-assembly of chiral gelator is described. Tuning of molecular chirality *in situ* triggers different assemblies of superstructures exhibiting fluorescence. This novel AIE material can constitute an emerging library of chiral supramolecules for turn-on fluorescent sensors. It will also help in better understanding the effects of chiral factors on the photophysical process.

Supramolecular self-assembly[1] is ubiquitous in nature; in addition, it plays crucial roles in drug delivery,[2] chiral separation,[3] and biosensing.[4] The understanding associated with the integration of self-assembled approaches to modified AIE-active fluorogenic molecules is a promising direction for the research on supramolecular materials and their optical applications,[5] which can be significantly extended to biological applications for which high concentrations are crucial. The integration of AIE with chiral self-assembled superstructures is attracting increasing attention because of their advantages.[6] Herein, a novel AIE phenomenon via the integration of chiral aggregated superstructures is described. C_3-symmetric molecules are used as the building blocks because their excellent framework can easily afford supramolecular gels via non-covalent interactions.[7] Upon chiral aggregation, nanofibers and micro-loops are formed on the mica surface. Moreover, the loop-like aggregates exhibit typical AIE characteristics attributed to multiple intermolecular interactions.[8]

In this study, a pair of dipeptide sequences (L-Asp-L-Phe and D-Asp-D-Phe) were chosen as the fundamental unit because of their multiple hydrogen bonding sites and chiral centers, which were crucial for the regulation of assembly modes.[9] The 1, 3, 5-trisubstituted phenyl group was introduced as the core for constructing the C_3-symmetric trefoil-like structure (Fig. 1). First, L-Asp-L-Phe and D-Asp-D-Phe were prepared by solid-phase peptide synthesis (SPPS). L,L-G1 and D,D-G1 were then synthesized in 78% yield (Fig. S1, ESI†). Both L,L-G1 and D,D-G1 formed macroscopic organogels in methanol, with their microstructures containing three-dimensional cross-linked fibers (Fig. S2, ESI†).

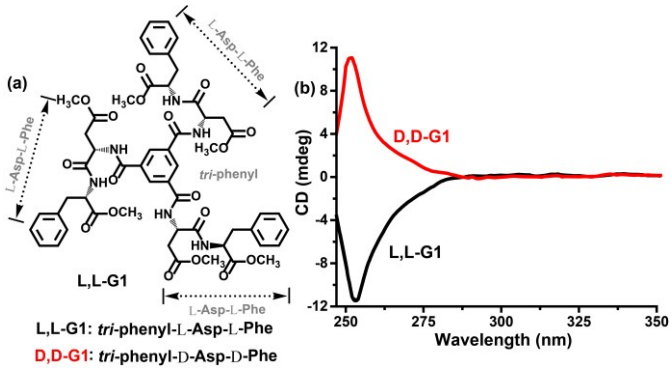

Fig. 1 Chemical structure (a) and circular dichroism spectra (b) of a pair of C_3-symmetric molecules (10^{-5} M in ethyl acetate, 25 ℃).

Interestingly, L,L-G1 and D,D-G1 exhibited contrasting micropatterns in ethyl acetate (Fig. S3, ESI†). As shown in the atomic force microscope (AFM) images in Fig. 2, long, twinning fibers and isolated micro-loops were clearly observed on the mica surface, indicating that chiral signals has been transferred from a single-molecule level to a supramolecular scale.[10] An average height of 5nm was observed for L,L-G1 aggregates (Fig. 2a), typical of coiled superhelix structures. These intertwined "tape reels" appeared to be rolled from a single fiber into several spiral ribbons by hierarchical self-assembly. However, the D,D-G1 aggregates exhibited an unusual type of a loop-like structure with an average height of 140 nm (Fig. 2b). Micro-loops with a diameter of 9 μm and a thickness of 400 nm were

[a] State Key laboratory of Advanced Technology for Materials Synthesis and Processing, Wuhan University of Technology, Wuhan, 430070, China.
[b] School of Chemistry, Chemical Engineering and Life Science, Wuhan University of Technology, 122 Luoshi Road, Wuhan, 430070, China.
* E-mail: suntl@whut.edu.cn
†Electronic Supplementary Information (ESI) available: experimental details, characterization, macroscopic organogel images, AFM images, SEM images, ATR-FTIR, nano-FTIR, and s-SNOM tests.
See DOI: 10.1039/x0xx00000x
‡ These authors contributed equally to this work

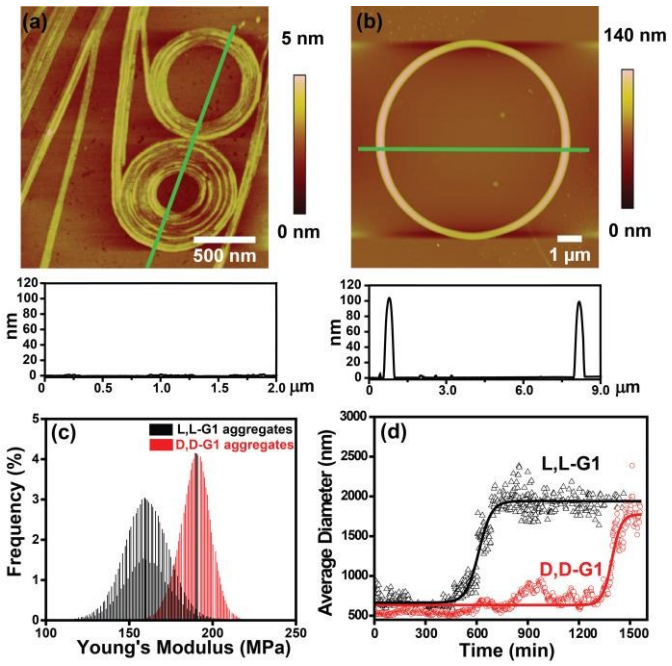

Fig. 2 AFM images of the aggregates on mica substrates in the tapping mode: (a) L,L-G1; (b) D,D-G1; Young's modulus of aggregates measured by AFM in the PeakForce QNM mode (c); and the dynamic assembly of L,L-G1 and D,D-G1 observed by dynamic light scattering (DLS) measurements (d).

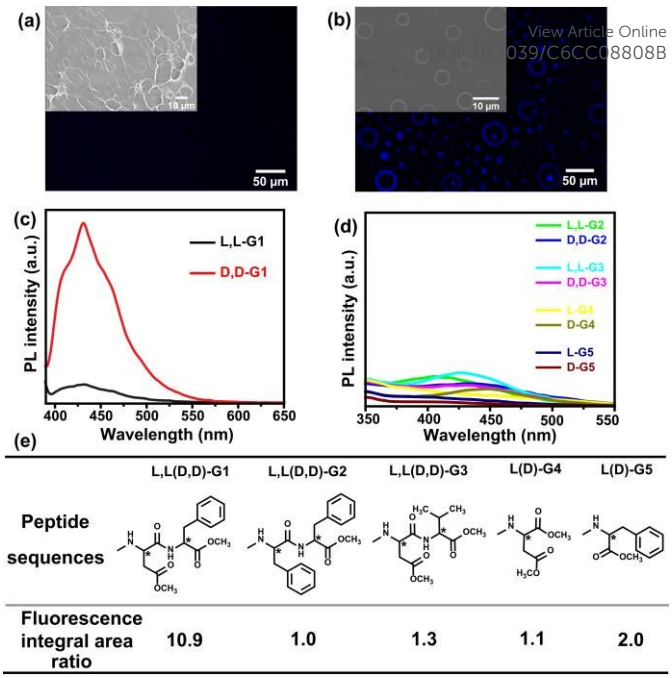

Fig. 3 Fluorescence microscopy images of L,L-G1 aggregates (a) and D,D-G1 aggregates (b), Insets: SEM images of the superstructures obtained on gold-coated mica surface; PL spectra of L,L(D,D)-G1 (c) and L,L(D,D)-G2 to L(D)-G5 (d) in ethyl acetate; and fluorescence integral area ratio for the selected ten molecules with different peptide sequences (e). Concentration: 10^{-4} M, λ_{ex}: 370 nm

also observed, which was consistent with scanning electron microscopy (SEM) images (Fig. S4, ESI†). This result suggested that the layer-by-layer assembly of micro-loops. Hence, for L,L-G1, once elementary nanofibers coiled to form a superhelix in a hierarchical manner, it is thought that these nanofibers pack into significantly large supercoiled structures. Meanwhile, D,D-G1 possibly assembled "layer by layer," thereby forming layers of periodically stacked patterns. Previously, π–π stacking interactions among phenyl groups have been reported to be one of the key factors responsible for periodically stacking micropatterns.[11]

The mechanical properties of aggregates were examined by AFM in the PeakForce Quantitative Nanomechanical Mapping (QNM) mode, which allows for quantitative nanomechanical mapping of the Young's modulus. The elastic modulus can be calculated from the Derjaguin, Muller, Toropov model, which is a direct measure of the surface hardness of samples.[12] The average Young's modulus value for the micro-loops and nanofibers were approximately 190 MPa and 160 MPa, respectively (Fig. 2c). These results indicated that as compared to fiber-like aggregates, the loop-like aggregates in D,D-G1 are assembled more compactly. To further explore this difference in assembly, dynamic light scattering (DLS) measurements were conducted to monitor the kinetic process at room temperature. The apparent hydrodynamic radius was calculated using the Stokes-Einstein equation,[13] several measurements were performed for each sample to obtain an average hydrodynamic radius. The initiation time of micro-loops was twice that of the fibers (Fig. 2d), implying that the construction of fine D,D-G1 superstructures takes a longer time than that required to construct random nanofibers.

Surprisingly, both the microstructures emitted dissimilar fluorescence signals. As shown in the dark-field image in Fig. 3a, L,L-G1 aggregates did not exhibit any remarkable fluorescence. However, a network of fiber bundles or ropes composed of thin fibers was clearly observed in the SEM images. By contrast, in D,D-G1 aggregates, several micro-loops exhibited bright blue fluorescence. The diameter of those loops ranged from 5 μm to 40 μm, because of the dynamic stages of aggregation, as shown in the SEM images. Interestingly, non-conjugated molecules (such as D,D-G1) exhibited typical AIE behavior (Fig. 3c). Furthermore, the micropatterns switched from non-emissive fibers to emissive loop-like aggregates because of chiral inversion. The nanostructures and PL emissions of the mixed L,L-G1 and D,D-G1 in various ratios were also investigated (Fig. S5, ESI†). With the increase of D,D-G1 percentage, PL intensity increased with the D,D-G1 ratio rising and entangled nanofibers gathered. First, those loops appeared above the fibers' surface with an average height of 64 nm. Then the quantity of fibers decreased and micro-loop increased as the typical patterns to be observed. When D,D-G1 ratio was 100%, no fibers existed except for loops of varying sizes. These results further demonstrates the "layer by layer" assembled way for D,D-G1 and reflects the immense potential of this AIE material for applications for biological detection via specific recognition.

Furthermore, substituent replacement was carried out to investigate the relationship between peptide sequences and fluorescence discrimination during aggregate formation. Eight peptide sequences were examined (Fig. 3d, e): L-Phe-L-Phe (L,L-G2); D-Phe-D-Phe (D,D-G2); L-Asp-L-Val (L,L-G3); D-Asp-D-Val

(D,D-G3); L-Asp (L-G4); D-Asp (D-G4); L-Phe (L-G5); and D-Phe (D-G5). First, Phe was used to replace the Asp residue, affording a rigid sequence with strong π–π interactions. Neither L,L-G2 nor D,D-G2 exhibited clear emissions, indicating that excessive π–π interactions possibly inhibit radiative decay; this inhibition can result in aggregation-caused quenching (ACQ). Next, the Phe residue was replaced with Val (Valine), to obtain a flexible sequence. Interestingly, the fluorescence discrimination ratio was slightly greater than that of a Phe-Phe sequence, indicative of the involvement of hydrogen bonding. Control experiments were conducted using a single-arm peptide based on Asp-Phe. The discrimination ratio of L(D)-G4 was less than that of L,L(D,D)-G3, indicating that multiple hydrogen bonds can promote dissimilar light emission behavior. The discrimination ratio of L(D)-G5 with a single Phe arm was two times as high as that of L,L(D,D)-G2, suggesting that appropriate π–π stacking can effectively increase the optical emission gap. The Phe residue is confirmed to be crucial for light-emission, and the presence of Asp promotes this process. Hence, when coupled with limited π–π stacking, multiple hydrogen bonding can cooperatively contribute to the contrasting fluorescence emission characteristics, similar to that observed for L,L-G1 and D,D-G1. The self-assembled nanostructures of these eight molecules were also investigated (Fig. S6, ESI†). These results not only confirmed the significant contribution of Asp and Phe residues to the AIE phenomenon, but also revealed that loop-like, optically active aggregates of D,D-G1 are possibly related to stereoselective interactions. This assumption can be further explained with the use of restricted intramolecular motion (RIM).[14] In D,D-G1 assemblies, congested phenyl-packing can block the motion of intramolecular bonds, leading to remarkable enhancement of luminescence.[15] Recently, Liu et al.[16] have reported a C_3-symmetric molecule self-assembled into optically active supramolecular gels. The results obtained herein are in agreement with their results in terms of the growth of the hierarchical aggregates exhibiting chiral conformation, generating different optical effects with macroscopic chirality.

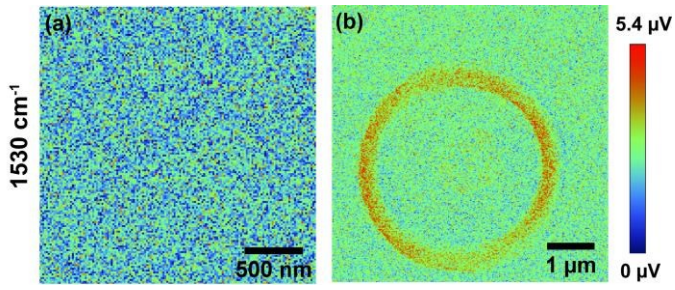

Fig. 4 Infrared near-field images of aggregates at 1530 cm^{-1}: (a) L,L-G1; (b) D,D-G1.

To further explore this phenomenon, Fourier transform infrared nanospectroscopy (nano-FTIR) using a scattering-type scanning near-field optical microscope (s-SNOM) was employed to investigate the involvement of functional groups in these two aggregates. The analysis of amide bands provides notable insights into the secondary structures of peptides or proteins.[17] Hence, the attenuated total reflection (ATR)-FTIR spectrum of monomeric samples is recorded (Fig. S7a, ESI†) to measure the amide I and II bands in the range 1400—1700 cm^{-1}. Similar peaks were observed for both monomeric L,L-G1 and D,D-G1. From the nano-FTIR spectrum of their aggregates in the supramolecular state (Fig. S7b, ESI†), strong peaks were observed at 1530 and 1657cm^{-1} in the spectrum of D,D-G1 aggregates. The peak at 1530 cm^{-1} could be ascribed to NH deformation and CN stretching vibrations (the amide band II region), while the peak at 1657 cm^{-1} could be attributed to CO stretching vibrations (the amide band I region). However, peaks in the L,L-G1 aggregates (only 1657 cm^{-1}) were weaker than those observed for D,D-G1, demonstrating that only CO stretching vibrations participate in fiber-like aggregation.

To visualize the nanoscale distribution of functional groups, s-SNOM imaging was employed within a range of frequencies using a tunable quantum cascade laser (QCL). The IR near-field images of the loop-like aggregates and thin fibrils were clearly different at the two wavenumbers. The micro-loop was clearly observed at 1530 cm^{-1} (Fig. 4b). However, it was difficult to observe the nanofibers (Fig. 4a). At 1657 cm^{-1}, a fiber structure was observed (Fig. S7c, ESI†), and micro-loops exhibited relatively strong signals (Fig. S7d, ESI†). This observation indicated that only the hydrogen bonding motif of the C=O group participates in the fiber-like assembly. However, the micro-loop aggregates were associated with multiple hydrogen bonds. Assuming that C_3-symmetric molecules can form supramolecular stacks, the central aromatic bridge with three phenyl rings is hypothesized to exhibit strong π–π interactions. Both multiple hydrogen bonding and π–π interactions cooperatively contributed to the loop-like aggregates to some degree. The presence of C=O hydrogen bonds can possibly explain the self-association of fibrils.

In summary, an interesting AIE phenomenon was discovered, confirming that discrimination by chiral self-assembly affects fluorescence emission. Novel luminescent micro-loops were constructed by the assembly of the D-Asp-D-Phe methyl-ester-modified C_3-symmetric molecule. This exquisite bottom-up fabrication via non-covalent molecular interactions of molecules is efficient for constructing novel nanomaterials with specific superstructures and enhanced emission characteristics. Loop-like, fiber-like aggregates exhibit different alignment modes, based on π–π stacking interactions and intermolecular hydrogen bonds. The optically active aggregates are possibly formed by steric hindrance, resulting from overcrowded packing of molecules. These results provide interesting insight into the combination of AIE characteristics and chiral self-assembled structures. Exploring the chiral factor and the involved non-covalent interactions may help in better understanding the fundamental mechanism during supramolecular self-assembly, as well as their resultant optical capabilities. This may lead to innovations, such as improvement in the rational molecular design, thereby expanding the application areas of biological detection[18] and electroluminescence devices.[19]

This work was sponsored by the Major State Basic Research Development Program of China (973 Program) (No. 2013CB933002), the China National Funds for Distinguished Young Scientists (No. 51325302) and the National Natural Science Foundation of China (No. 21275114, 51473131). G. Qing acknowledges Hubei Provincial Department of Education for financial assistance through the "Chutian Scholar" Program and Hubei Provincial Natural Science Foundation of China (No. 2014CFA039).

Notes and references

1 (a) J. M. Lehn, *Science*, 2002, **295**, 2400; (b) S. De Feyter and F. C. De Schryver, *Chem. Soc. Rev.*, 2003, **32**, 139; (c) J. W. Steed, *Chem. Commun.*, 2011, **47**, 1379; (d) T. Aida, E. W. Meijer and S. I. Stupp, *Science*, 2012, **335**, 813.

2 (a) P. K. Vemula and G. John, *Acc. Chem. Res.*, 2008, **41**, 769. (b) X. Zhang and C. Wang, *Chem. Soc. Rev.*, 2011, **40**, 94. (c) R. Dong, S. P. Ravinathan, L. Xue, N. Li, Y. Zhang, L. Zhou, C. Cao and X. Zhu, *Chem. Commun.*, 2016, **52**, 7950.

3 (a) M. O. Lorenzo, C. J. Baddeley, C. Muryn and R. Raval, *Nature*, 2000, **404**, 376. (b) K. E. Shopsowitz, H. Qi, W. Y. Hamad and M. J. MacLachlan, *Nature*, 2010, **468**, 422.

4 (a) R. J. William, A. M. Smith, R. Collins, N. Hodson, A. K. Das and R. V. Ulijn, *Nat. Nanotech.*, 2009, **4**, 19. (b) M. H. Lee, J. Y. Kim, J. H. Han, S. Bhuniya, J. L. Sessler, C. Kang and J. S. Kim, *J. Am. Chem. Soc.*, 2012, **134**, 12668.

5 (a) J. Luo, Z. Xie, J. W. Y. Lam, L. Cheng, H. Chen, C. Qiu, H. S. Kwok, X. Zhan, Y. Liu, D. Zhu and B. Z. Tang, *Chem. Commun.*, 2001, 1740. (b) Y. Hong, J. W. Y. Lam and B. Z. Tang, *Chem. Commun.*, 2009, 4332. (c) Y. Hong, J. W. Y. Lam and B. Z. Tang, *Chem. Soc. Rev.*, 2011, **40**, 5361.

6 (a) A. Kuzyk, R. Schreiber, Z. Fan, G. Pardatscher, E. M. Roller, A. Högele, F. C. Simmel, A. O. Govorov and T. Liedl, *Nature*, 2012, **483**, 311. (b) K. Liu, Y. Yao, Y. Kang, Y. Liu, Y. Han, Y. Wang, Z. Li and X. Zhang, *Sci. Rep.*, 2013, **3**, 2372.

7 (a) S. Cantekin, T. F. de Greef and A. R. Palmans, *Chem. Soc. Rev.*, 2012, **41**, 6125. (b) S. Y. Ryu, S. Kim, J. Seo, Y.W. Kim, O. H. Kwon, D. J. Jang and S. Y. Park, *Chem. Commun.*, 2004, 70. (c) F. Aparicio, F. García and L. Sánchez. *Chem. - Eur. J.*, 2013, **19**, 3239. (d) J. J. van Gorp, J. J. M. Vekemans and E.W.Meijer, *J. Am. Chem. Soc.*, 2002, **124**, 14759.

8 (a) K. S. Mali, K. Lava, K. Binnemans and S. De Feyter, *Chem. - Eur. J.*, 2010, **16**, 14447. (b) M. Alajarin, R. A. Orenes, J. W. Steed and A. Pastor, *Chem. Commun.*, 2010, **46**, 1394. (c) X. Yan, S. Li, J. B. Pollock, T. R. Cook, J. Chen, Y. Zhang, X. Ji, Y. Yu, F. Huang and P. J. Stang, *Proc. Natl. Acad. Sci. U. S. A.*, 2013, **110**, 15585. (d) M. H. Lee, J. S. Kim and J. L. Sessler, *Chem. Soc. Rev.*, 2015, **44**, 4185.

9 G. Qing, X. Shan, W. Chen, Z. Lv, P. Xiong and T. Sun, *Angew. Chem. Int. Ed.*, 2014, **53**, 2124.

10 (a) G. Qing and T. Sun, *NPG Asia Mat.*, 2012, **4**, e4. (b) X. Yan, F. Wang, B. Zheng and F. Huang, *Chem. Soc. Rev.*, 2012, **41**, 6042. (c) J. Xu, L. Chen and X. Zhang, *Chem.-Eur. J.*, 2015, **21**, 11938. (d) R. Garifullin and M. O. Guler, *Chem. Commun.*, 2015, **51**, 12470.

11 (a) A. Kuzyk, R. Schreiber, Z. Fan, G. Pardatscher, E. M. Roller, A. Högele, F. C. Simmel, A. O. Govorov and T. Liedl, *Nature*, 2012, **483**, 311. (b) N. Na, X. Mu, Q. Liu, J. Wen, F. Wang and J. Ouyang, *Chem. Commun.*, 2013, **49**, 10076.

12 B. V. Derjaguin, V. M. Muller and Yu. P. Toporov, *J. Colloid Interf. Sci.*, 1975, **53**, 314.

13 (a)A. Einstein, *Ann. Physik*, 1905, **17**, 549. (b) G. Stokes. *Trans. Cambridge Phil. Soc.*, 1856, **9**, 5.

14 (a) L. Zong, Y. Xie, C. Wang, J. Li, Q. Li and Z. Li, *Chem. Commun.*, 2016, **52**, 11496. (b) W. Bai, Z. Wang, J. Tong, J. Mei, A. Qin, J. Z. Sun and B. Z. Tang, *Chem. Commun.*, 2015, **51**, 1089. (c) S. Xu, X. Zhang, C. Nie, Z. Pang, X. Xu and X. Zhao, *Chem. Commun.*, 2015, **51**, 16417.

15 (a) Y. Qian, S. Li, G. Zhang, Q. Wang, S. Wang, H. Xu, C. Li, Y. Li and G. Yang, *J. Phys. Chem. B*, 2007, **111**, 5861. (b) T. Mutai, H. Sawatani, T. Shida, H. Shono and K. Araki, *J. Am. Chem. Soc.*, 2013, **78**, 2482. (c) M. Kang, P. Zhang, H. Cui and S. M. Loverde, *Macromolecules*, 2016, **49**, 994.

16 Z. Shen, T. Wang and M. Liu, *Angew. Chem. Int. Ed.*, 2014, **126**, 13642.

17 (a) I. Amenabar, S. Poly, W. Nuansing, E. H. Hubrich, A. A. Govyadinov, F. Huth, R. Krutokhvostov, L. Zhang, M. Knez, J. Heberle, A. M. Bittner and R. Hillenbrand, *Nat. Commun.*, 2013, **4**, 2890. (b) H. A. Bechtel, E. A. Muller, R. L. Olmon, M. C. Martin and M. B. Raschke, *Proc. Natl. Acad. Sci. U. S. A.*, 2014, **111**, 7191.

18 (a) L. Hsu, G. L. Cvetanovich and S. I. Stupp, *J. Am. Chem. Soc.*, 2008, **130**, 3892. (b)C. Zhu, S. Pang, J. Xu, L. Jia, F. Xu, J. Mei, A. Qin, J. Sun, J. Ji and B. Z. Tang, *Analyst*, 2011, **136**, 3343. (c) V. M. Suresh, A. De and T, K. Maji, *Chem. Commun.*, 2015, **51**, 14678.

19 (a) S. Zhang, A. Qin, J. Sun and B. Z. Tang, *Prog. Chem.*, 2011, **23**, 623. (b) B. Wang, Y. Wang, J. Hua, Y. Jiang, J. Huang, S. Qian and H. Tian, *Chem. - Eur. J.*, 2011, **17**, 2647. (c) G. Yu, G. Tang and F. Huang, *J. Mater. Chem. C*, 2014, **2**, 6609.